

DESY 11-229  
SFB/CPP-11-72  
LPN11-68

# Neutral triple electroweak gauge boson production in the large extra-dimension model at the LHC

M. C. Kumar<sup>a,1</sup>    Prakash Mathews<sup>b,2</sup>    V. Ravindran<sup>c,3</sup>    Satyajit Seth<sup>b,4</sup>

<sup>a</sup> Deutsches Elektronen-Synchrotron DESY, Platanenallee 6, D-15738 Zeuthen, Germany

<sup>b</sup> Saha Institute of Nuclear Physics, 1/AF Bidhan Nagar, Kolkata 700 064, India

<sup>c</sup> Regional Centre for Accelerator-based Particle Physics  
Harish-Chandra Research Institute, Chhatnag Road, Jhansi,  
Allahabad 211 019, India

## Abstract

We study the prospects of probing large extra dimension model at the LHC through neutral triple gauge boson production processes. In theories with extra dimensions these processes result from the exchange of a tower of massive graviton modes between the SM particles. We consider  $\gamma\gamma\gamma$ ,  $\gamma\gamma Z$ ,  $\gamma ZZ$  and  $ZZZ$  production processes, and present our results for various kinematic distributions at the LHC for  $\sqrt{S} = 14$  TeV.

PACS number: 12.38.Bx, 13.85.Qk, 14.70.Hp, 14.80.Rt

---

<sup>1</sup>kumar.meduri@desy.de

<sup>2</sup>prakash.mathews@saha.ac.in

<sup>3</sup>ravindra@hri.res.in

<sup>4</sup>satyajit.seth@saha.ac.in

# 1 Introduction

The results that would emerge from the Large Hadron Collider (LHC) are expected to reveal patterns under which the standard model (SM) is likely to be modified at the TeV scale. At these high energies, LHC is expected to unveil the mystery of large hierarchy between the electroweak and the Planck scales and also produce interesting new physics signals. Two well-studied scenarios of physics beyond the SM at the TeV scale are extra dimension theories and supersymmetry, which will be tested at the LHC among many others. The large extra dimension model, proposed by Arkani-Hamed, Dimopoulos and Dvali (ADD) [1], circumvents the hierarchy problem by exploiting the geometry of extra spatial dimensions to find a mechanism to lower the Planck scale. The tower of Kaluza-Klein (KK) modes as a result of gravity propagating the full  $4+d$ -dimensions would mediate scattering processes and hence lead to deviations from the SM predictions. At colliders, exchange of virtual KK modes or emission of real KK modes give rise to interesting phenomenological signals at the TeV scale [2, 3]. Virtual effects of KK modes lead to the enhancement of the cross section of pair production in processes *viz.* di-lepton, di-gauge boson ( $\gamma\gamma$ ,  $ZZ$ ,  $W^+W^-$ ), dijet [4, 5, 6, 7, 8] in some kinematic regions. The real emission of KK modes leads to large missing  $\cancel{E}_T$  signals *viz.* mono jet, mono photon, mono Z boson and mono  $W^\pm$  boson [9].

The di-gauge boson final states have been extensively studied in the context of extra dimension models. The triple gauge boson final state is an interesting new physics signal in some of the beyond SM scenarios [10]. In this paper we consider the neutral triple gauge boson production at the LHC and study how the ADD model would alter the SM expectation. In the SM, the triple gauge boson final state is an important signal as it depends on the 3-point and 4-point couplings among the gauge bosons which is a test of the electroweak theory. This process in the SM has been studied to leading order (LO) [11, 12] and its extension to the next to leading order (NLO) was on the Les Houches wish list [10] and has been finally achieved recently [13, 14, 15, 16]. The triple gauge boson production processes in the SM are the precise predictions of the electroweak gauge theory and gauge self-couplings. They are also potential background to many new physics models like supersymmetry and Technicolor. For example,  $Z\gamma\gamma$  in SM is a background to signals with di-photons and missing transverse energy in gauge mediated super symmetric theories [17] and  $\gamma\gamma\gamma$  production in SM is a background to one photon plus techni-pion [18]. Processes with three gauge bosons can also come from the ADD model as gravitons couple directly to gauge bosons of SM. While mono-jet or di-lepton production is more sensitive to parameters of models with extra-dimensions compared to the triple gauge boson production, all these processes involve same universal coupling of gravity with the SM particles, and hence can provide equally important information about the model. Moreover, in discriminating physics beyond the SM namely SUSY or technicolour models using triple gauge boson production, one can not ignore the potential contributions resulting from models with extra dimensions.

In this analysis we consider the process  $PP \rightarrow VVV X$ , where we restrict to the neutral gauge bosons  $V = \gamma, Z$  and  $X$  is some hadronic final state. The following four final states are the subject of this analysis: (i)  $\gamma\gamma\gamma$  (ii)  $\gamma\gamma Z$  (iii)  $\gamma ZZ$  and (iv)  $ZZZ$ . The case where  $V = W^\pm$  will be part of a different paper [19].

This paper is organised as follows: in section 2 we present the analytical calculation of the above mentioned processes with a brief introduction to the ADD model, section 3 is arranged to present the numerical results of our studies and finally we summarise the results in the last section.

## 2 Neutral triple gauge boson production

The TeV scale colliders like the LHC are suitable for studying the quantum gravity effects in the ADD model. This model is defined in such a way that the SM particles are localised on a 3-brane with negligible tension and only gravity can propagate in the full  $4 + d$  dimensions as it describes the geometry of the full space time. The extra spatial dimensions  $d$  can be compactified on a  $d$ -dimensional torus with a common radius  $R/(2\pi)$  of macroscopic size. As a consequence, the effective Planck scale ( $M_P$ ) in 4 space-time dimensions is related to the fundamental Planck scale ( $M_S$ ) in  $4 + d$  dimensions as follows,

$$M_P^2 = C_d M_S^{2+d} R^d , \quad (1)$$

where  $C_d = 2(4\pi)^{-\frac{d}{2}}/\Gamma(d/2)$ . Although, the SM particles are localised on a 3-brane, they can sense the extra dimensions by their interaction with gravity via the massive KK towers of the graviton. The corresponding interaction Lagrangian is the following,

$$\mathcal{L} = -\frac{\kappa}{2} \sum_{\vec{n}=0}^{\infty} T^{\mu\nu}(x) h_{\mu\nu}^{\vec{n}}(x) , \quad (2)$$

where  $\kappa = \sqrt{16\pi}/M_P$ ,  $T^{\mu\nu}$  is the energy-momentum tensor of localised SM fields and  $h_{\mu\nu}^{\vec{n}}$  denotes the massive KK graviton labeled by a  $d$ -dimensional vector  $\vec{n}$  with all positive components.  $h_{\mu\nu}^{\vec{n}}$  contains one spin-2 state,  $(n-1)$  spin-1 states and  $n(n-1)/2$  spin-0 states, having mass,

$$m_{\vec{n}}^2 = \frac{4\pi^2 \vec{n}^2}{R^2} . \quad (3)$$

The zero mode of the KK tower corresponds to the massless graviton in the 4 space-time dimensions. The effective graviton propagator, after summing over all KK states, can be expressed as,

$$\begin{aligned} \mathcal{D}_{eff}(s) &= \sum_{\vec{n}} \frac{1}{s - m_{\vec{n}}^2 + i\varepsilon} , \\ &= \frac{1}{\kappa^2} \frac{8\pi}{M_S^4} \left( \frac{\sqrt{s}}{M_S} \right)^{(d-2)} [\pi + 2iI(\Lambda/\sqrt{s})] , \end{aligned} \quad (4)$$

where  $s$  is the invariant mass of the boson pair resulting from the decay of the KK mode and the function  $I(\Lambda/\sqrt{s})$  is described in [3], which depends on the ultra violet cut-off  $\Lambda$ . Although the interaction of KK modes with the SM particles is suppressed by the coupling  $\kappa$  (Eq. (2)), the cumulative effect of summing over large number of accessible KK modes (Eq. (4)) compensates the suppression, making the effective coupling significant enough to have observable effects. It is usual practice to set the UV cutoff  $\Lambda = M_S$  and simplify the summation of virtual KK modes [2, 3] to do the phenomenology. We follow the approach of [3] for this analysis which retains the details of the number of extra dimensions.

The neutral gauge boson final state at the hadron collider  $PP \rightarrow VVV X$  at LO comes from the sub process

$$q(p_1) + \bar{q}(p_2) \longrightarrow V(p_3) + V(p_4) + V(p_5) \quad , \quad (5)$$

where  $V = \gamma, Z$  and  $X$  is any final state hadron. The SM diagram for the above process is shown in Fig. 1 with all possible permutations of final states. For the final state with at least two  $ZZ$ s, the Higgs could contribute by coupling to the quarks, but this is negligible in the vanishing quark mass limit. In the case of  $ZZZ$  final state, there are additional Higgs strahlung diagrams but their contribution is also quite small and vanishes in the large Higgs mass limit. Hence, we have not included the processes with the Higgs boson. In the ADD model, the KK modes couple to

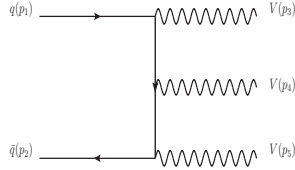


Figure 1: Typical Feynman diagram for triple gauge boson production in SM.

$V$  bosons, quarks, anti-quarks as well as to quark-antiquark- $V$  boson vertex. The four categories of Feynman diagrams that give a  $VVV$  final state in ADD model are shown in Fig. 2. We have used unitary gauge ( $\xi \rightarrow \infty$ ) for  $Z$ -boson and the Feynman gauge ( $\xi = 1$ ) for the photon.

In the SM, the LO process for the production of  $\gamma\gamma\gamma$  at hadron colliders results from the annihilation of a quark and an anti-quark. In the ADD model, the production mechanism is again from the same initial states but one of the photon comes from either quark or an antiquark and other two photons come from the decay of KK graviton. The typical Feynman diagrams that contribute in the SM and in the ADD model are shown in Fig. 1, 2. The Feynman rules for the processes with KK graviton can be found in [2, 3]. All the expressions for the matrix element squared with proper spin, color sums and averages are obtained using a symbolic program based on FORM [20]. The KK graviton propagator in the ADD model is proportional to

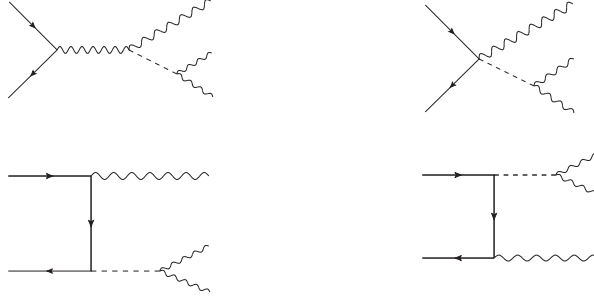


Figure 2: Typical Feynman diagrams for triple gauge boson production in ADD model. Dashed line represents the KK mode of the graviton and the other particle lines are same as in Fig. 1.

$\mathcal{D}$ ,

$$\mathcal{D} = \sum_{\vec{n}} \frac{1}{s_{ij} - m_{\vec{n}}^2 + i\varepsilon} , \quad (6)$$

where the invariants are  $s_{ij} = (p_i + p_j)^2$ , and  $\mathcal{D}$  can be evaluated using Eq. (4). The numerator of the spin-2 propagator [3] of the KK graviton is given by

$$B_{\mu\nu,\rho\sigma}(k) = \eta_{\mu\rho}\eta_{\nu\sigma} + \eta_{\mu\sigma}\eta_{\nu\rho} - \frac{2}{3}\eta_{\mu\nu}\eta_{\rho\sigma} , \quad (7)$$

where  $\eta_{\mu\nu} = g_{\mu\nu} - k_\mu k_\nu / m_{\vec{n}}^2$ . Here  $k$  is the momentum flowing through the propagator. Terms proportional to negative powers of mass of KK mode in  $\eta_{\mu\nu}$  do not contribute as they are proportional to  $k_\mu k_\nu$ . This provides a useful check on our calculation. The matrix elements have been checked for gauge invariance. We performed similar computation for evaluating the parton level subprocesses for  $\gamma\gamma Z$ ,  $\gamma ZZ$  and  $ZZZ$  productions. In the following we list few of the important observations.

For the  $\gamma\gamma Z$  production, in the limit  $m_Z \rightarrow 0$ , we reproduce the matrix elements for  $\gamma\gamma\gamma$  process with the changes:  $(C_V^2 + C_A^2)/4 \rightarrow Q_f^2$ ,  $T_z \rightarrow e$ , where  $C_V$ ,  $C_A$  are the vector and axial vector couplings of the weak gauge boson respectively,  $T_z = e/(\sin\theta_w \cos\theta_w)$  and  $Q_f$  is the electric charge of the quark flavors. In the case of  $\gamma ZZ$  production, we find that the parton level subprocesses in SM and ADD model are similar to those of the  $\gamma\gamma Z$  production with the changes  $\gamma \leftrightarrow Z$ . The squared matrix elements for  $\gamma ZZ$  production that come from ADD model alone are not related to those of  $\gamma\gamma\gamma$  production. The reason is that some of the terms proportional to  $m_Z^2$  that appear in the graviton- $ZZ$  vertex cancel all the inverse power of  $m_Z^2$  present in the  $Z$  boson polarisation sum, giving contributions that have no analogous ones in the  $\gamma\gamma\gamma$  process. However, the expression for SM squared matrix elements of  $\gamma ZZ$  is related to that of  $\gamma\gamma\gamma$  process in the SM if we take  $m_Z \rightarrow 0$ ,  $(C_V^4 + 6C_V^2 C_A^2 + C_A^4)/16 \rightarrow Q_f^4$  and  $T_z \rightarrow e$ . For  $ZZZ$  production, squared matrix elements involving ADD vertices do not have any relation with those of  $\gamma\gamma\gamma$

production for the same reason as  $\gamma ZZ$  production case. The SM squared matrix elements of this process are related to those for the  $\gamma\gamma\gamma$  process in SM with the following replacement<sup>5</sup> in the limit  $m_Z \rightarrow 0$ ,  $(C_V^6 + 15C_V^4C_A^2 + 15C_V^2C_A^4 + C_A^6)/64 \rightarrow Q_f^6$ ,  $T_z \rightarrow e$ . The expressions for the squared matrix elements of the processes discussed above are too large to be presented in this paper.

### 3 Numerical results

In this section, we present different kinematical distributions for the production of neutral triple gauge bosons. The predictions are for the LHC at center of mass energy  $\sqrt{S} = 14$  TeV. We have used CTEQ6L parton densities [21]. For the strong coupling constant that appears in CTEQ6L, we use  $\Lambda_{QCD} = 0.226$  GeV and  $n_f = 5$  flavors. We set the factorisation scale  $\mu_F = P_T^V$  for the transverse momentum distribution of  $V$  and  $\mu_F = Q$  for the invariant mass ( $Q$ ) distribution of the di-boson pair. In addition we apply the following cuts on  $P_T^V$  and the rapidity  $y^V$ :

$$P_T^{\gamma,Z} \geq 25 \text{ GeV} \quad \text{and} \quad y^{\gamma,Z} < 2.7. \quad (8)$$

We also ensure that in general the invariant mass of the di-boson (*i.e.* any two identical bosons among the 3V) is less than  $M_S$ . We use  $m_Z = 91.1876$  GeV and  $\sin^2 \theta_w = 0.2312$ . The fine structure constant is taken as  $\alpha = 1/128$ .

Recently, both CMS [22] and ATLAS [23] reported, searches for signatures of extra dimensions in the di-photon mass spectrum at the LHC for 7 TeV p p collisions. The 95 % lower bound on  $M_S$  vary between 2.27 - 3.53 TeV depending on the number of extra dimensions  $d = 7 - 3$  for ATLAS and  $M_S$  vary between 2.3 - 3.8 TeV depending on the number of extra dimensions  $d = 7 - 2$  for CMS, both using a fixed  $K$  factor of about 1.6 [6]. Hence we have used the phenomenologically viable ADD model parameters  $M_S = 3.5$  TeV and  $d = 3$  for present study.

For the processes involving more than one photon, it is important to isolate photons from each other *i.e.* they need to be well separated in phase space so that they can be identified as separate objects in the detector. To do this we consider a cone of radius  $R = \sqrt{(\Delta y)^2 + (\Delta \phi)^2}$  in the rapidity-azimuthal angle plane  $(y, \phi)$  and ensure that the minimum separation between any two photons is taken to be  $R_{\gamma\gamma} = 0.4$ . In the following, we describe our findings for the various triple gauge boson production processes.

1.  $\gamma\gamma\gamma$  production: In this case, the three photons in the final states are classified in such a way that  $P_T^{\gamma_1} > P_T^{\gamma_2} > P_T^{\gamma_3}$ . We have compared our predictions for  $P_T^{\gamma_1}$  distribution in the SM against those given in [16] and found a very good agreement confirming the correct implementation of our analytical results in our numerical code. In the left panel of Fig. 3, we present the transverse momentum distributions

---

<sup>5</sup>We find that the most general result for the replacement of  $n$  number of Z-boson with photon in the SM squared matrix element is  $\frac{(C_V^2 + C_A^2)^n + 2n(n-1)(C_V^2 C_A^2 (C_V^2 + C_A^2)^{n-2})}{4^n} \rightarrow Q_f^{2n}$ , which works for all the above three processes for  $n = 1, 2, 3$ .

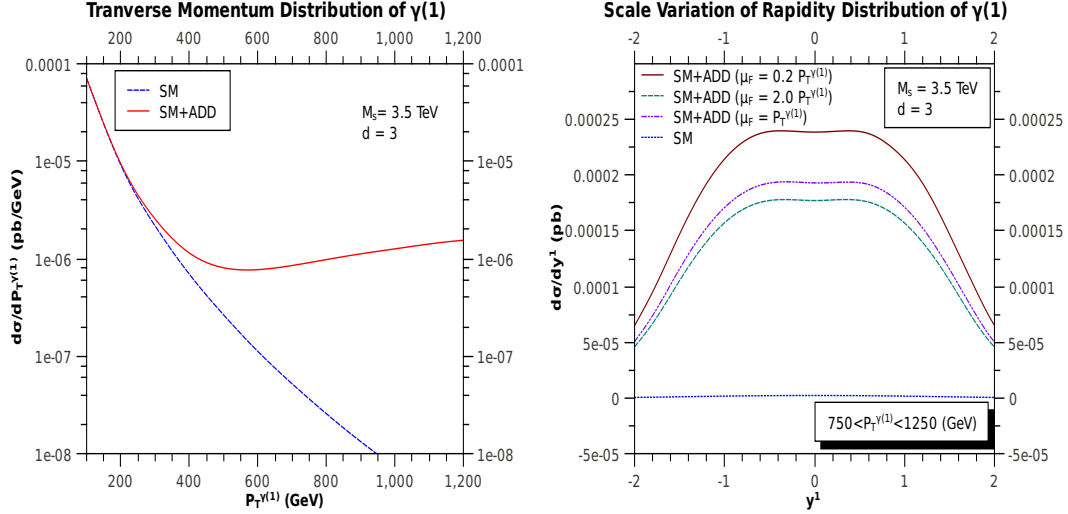


Figure 3: Transverse momentum distribution of  $\gamma_1$  [i.e, with maximum  $P_T$ ] (left panel) at the LHC for  $M_S = 3.5$  TeV and  $d = 3$ . Rapidity distribution of  $\gamma_1$  (right panel) at the LHC for ADD model parameters  $M_S = 3.5$  TeV and  $d = 3$  in the region where  $P_T^{\gamma_1} \in (750, 1250)$  GeV. Dependence of rapidity distribution of  $\gamma_1$  on the factorisation scale in the range  $\mu_F = 0.2 P_T^{\gamma_1}$  and  $\mu_F = 2 P_T^{\gamma_1}$ .

of  $\gamma_1$  in SM as well as in SM+ADD. We have chosen  $M_S = 3.5$  TeV and  $d = 3$  as representative parameters of the ADD model. In high  $P_T^{\gamma_1}$  region, the distribution for SM+ADD is fully controlled by processes coming from ADD model and is enhanced due to the dominant contributions of the KK modes. In the right panel of Fig. 3, rapidity distributions of the most energetic photon  $\gamma_1$  are shown for  $750 < P_T^{\gamma_1} < 1250$  GeV in SM and SM+ADD. It is seen that the SM contribution is extremely small in this range.

In order to estimate the factorisation scale  $\mu_F$  dependence present in our LO results, in the right panel of Fig. 3 we have plotted rapidity distributions for three different choices of  $\mu_F$  i.e.,  $\mu_F = (0.2, 1, 2) P_T^{\gamma_1}$ . In the central rapidity region the variation of the rapidity distribution with respect to the factorisation scale is the largest. With respect to the central choice of  $\mu_F = P_T^{\gamma_1}$ , the variation is about 23.6 % and 8.2 % for the choice of  $\mu_F = 0.2 P_T^{\gamma_1}$  and  $\mu_F = 2 P_T^{\gamma_1}$  respectively.

The  $P_T$  distribution of  $\gamma_2$  is found to be similar to that of  $\gamma_1$ , but is different for  $\gamma_3$  (the least energetic of the three photons) as shown in Fig. 4 (left panel). Similarly its rapidity distribution Fig. 4 (right panel) is also different from the most energetic photon.

2.  $\gamma\gamma Z$  production: Here, the invariant mass distribution of the photon pair is a useful observable because in the ADD model the photon pair is one of the clean decay modes of the KK graviton and in the region of interest, this could give an enhancement of the tail of the distribution. In Fig. 5 (top left panel) we have presented the invariant mass distributions of the photon pair for different choices of

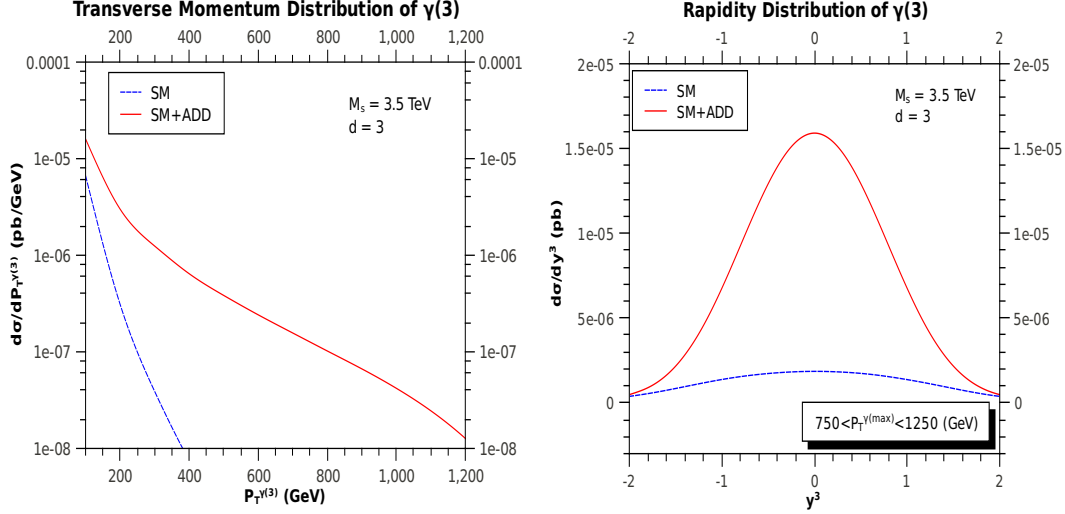


Figure 4: Transverse momentum distribution of  $\gamma_3$  [i.e, with minimum  $P_T$ ] (left panel) at the LHC for  $M_S = 3.5$  TeV and  $d = 3$ . Rapidity distribution of  $\gamma_3$  (right panel) at the LHC for  $M_S = 3.5$  TeV and  $d = 3$  in the region where  $P_T^{\gamma_3} \in (750, 1250)$  GeV.

$M_S = (3.5, 4, 4.5)$  TeV fixing  $d = 3$ , while in the top right panel the same distribution is plotted for different choices of  $d = 3, 4, 6$  but a fixed  $M_S = 3.5$  TeV. We find that the KK modes dominate over the SM contribution for larger values of invariant masses (say above 400 GeV for a given set of  $M_S$  and  $d$  values) of photon pairs leading to a significant enhancement of the signal over the background. We plot the factorisation scale dependence of invariant mass distributions of photon pairs in Fig. 6 (left panel) for different choices of  $\mu_F$ , i.e.,  $\mu_F = (0.2, 2)Q$ .

3.  $\gamma ZZ$  production: Invariant mass of Z boson pair is again a useful observable. We have done a similar analysis as we did for  $\gamma\gamma Z$  and use the same choice of factorisation scale and ADD model parameters. The invariant mass distributions are shown in the lower panels of Fig. 5 for different choices of  $M_S$  and  $d$ . We find that the invariant mass distributions of photon pairs in  $\gamma\gamma Z$  production and Z boson pairs here have similar qualitative behavior. In order to investigate the uncertainty resulting from the factorisation scale  $\mu_F$ , in Fig. 6 (right panel), we have plotted the invariant mass distributions of Z pairs for different choices of  $\mu_F$ , i.e.,  $\mu_F = (0.2, 2)Q$ .

4.  $ZZZ$  production: We have classified the triple Z-bosons in such a way that  $P_T^{Z_1} > P_T^{Z_2} > P_T^{Z_3}$  and for the  $P_T^{Z_i}$  distribution we make the choice of factorisation scale  $\mu_F = P_T^{Z_i}$ . In Fig. 7, we have presented the transverse momentum distributions of  $Z_1$  (left panel) and  $Z_3$  (middle panel) and rapidity distribution of  $Z_1$  (right panel) for SM and SM+ADD with  $M_S = 3.5$  TeV and  $d = 3$ . For the rapidity distribution, we have constrained  $900 < P_T^{Z_1} < 1400$  GeV. As in the case of  $\gamma\gamma\gamma$ , the  $P_T^{Z_2}$  distribution is similar to that of  $P_T^{Z_1}$  distribution. We have also shown the sensitivity of rapidity distribution to the factorisation scale  $\mu_F$  by varying between  $\mu_F = 0.2P_T^{Z_1}$



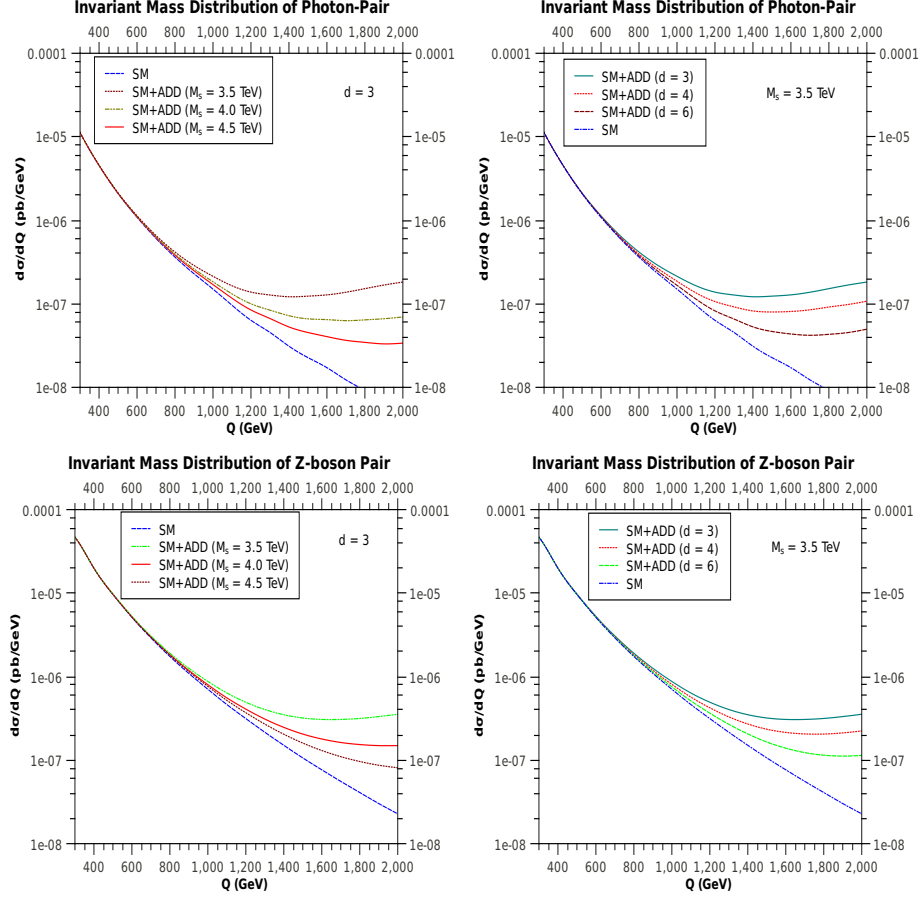


Figure 5: Invariant mass distribution of the photon pair (top left panel) and Z boson pair (bottom left panel) at the LHC for  $d = 3$  with different values of  $M_S$ . For  $M_S = 3.5$  TeV with different values of  $d$ , the invariant mass distribution of the photon pair (right top panel) and Z pair (right bottom panel).

and  $\mu_F = 2P_T^{Z_1}$ . In the central rapidity region we estimate the variation of the rapidity distribution with the factorisation scale and find that for  $\mu_F = 0.2P_T^{Z_1}$  and  $\mu_F = 2P_T^{Z_1}$ , the variation is about 27.5 % and 8.9 % respectively with respect to  $\mu_F = P_T^{Z_1}$ . The rapidity distribution for  $Z_2$  is similar to that of  $Z_1$  while  $Z_3$  is different.

5. Total cross section: The total cross sections for various processes involving neutral triple gauge boson final states as a function of  $M_S$  for a fixed value of  $d = 2$  are given in Fig. 8. The SM contributions that do not depend on ADD model parameter  $M_S$  appear as horizontal lines.

So far in our numerical analysis we have put the UV cutoff  $\Lambda = M_S$  which is the conventional choice to do the phenomenology. The sensitivity of the choice of UV cutoff is presented in Fig. 9 for  $P_T^{\gamma_1}$  distribution of  $\gamma\gamma\gamma$  final state and also the invariant mass distribution of  $\gamma\gamma$  pair of  $\gamma\gamma Z$  process by varying  $\Lambda = (0.9, 0.95, 1)M_S$ .

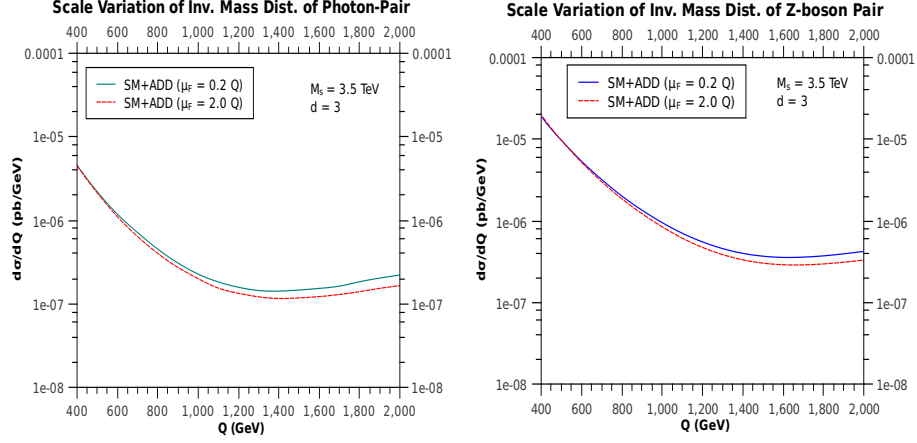


Figure 6: Dependence of invariant mass distribution of the photon pair (left panel) on factorisation scale at the LHC for  $d = 3$  and  $M_S = 3.5$  TeV. Dependence of invariant mass distribution of Z boson pair (right panel) on factorisation scale at the LHC for  $d = 3$  and  $M_S = 3.5$  TeV.

The cross section at  $P_T^{\gamma 1} = 1200$  GeV varies between 10 - 24 % as we vary  $\Lambda = (0.9, 0.95)M_S$  as compared to  $\Lambda = M_S$  for the  $\gamma\gamma\gamma$  process. Similarly the cross section for  $\gamma\gamma Z$  process at  $Q = 2000$  GeV the variation is 7 - 15 % in the same range of  $\Lambda$ .

The SM integrated K-factor for the  $\gamma\gamma\gamma$  process is about 2.6 and for  $\gamma\gamma Z$  it is 1.5 and these are larger than uncertainties resulting from the factorization scale variations at LO [16]. This warrants a full next to leading order QCD analysis which is beyond the scope of this paper. Such an analysis is reserved for future publication [24].

## 4 Conclusion

In this paper, we have studied the neutral triple gauge boson production at the LHC in theories with large extra dimensions which are produced via the exchange of a tower of KK graviton taking into account the SM contributions. All the final state photons and Z-bosons are taken to be real. We have performed various checks on our analytical results, and the numerical predictions are obtained using a Monte Carlo code which allows us to implement various experimental cuts. Our code has also been tested to reproduce SM transverse momentum distribution of the largest transverse momentum for the  $\gamma\gamma\gamma$  process. For the case in which the gauge bosons in the final state are identical we have presented the transverse momentum distribution by ordering the transverse momentum as  $P_T^1 > P_T^2 > P_T^3$ . We find that  $P_T^1$  and  $P_T^2$  distributions are similar but the one for  $P_T^3$  is different. The rapidity distributions are also presented. For the case where one of the gauge bosons in the final state is

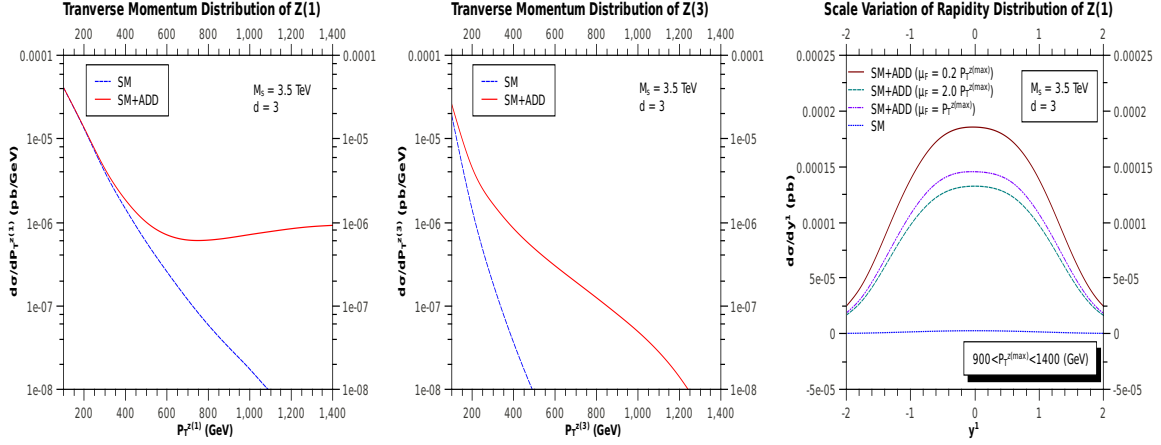


Figure 7: Transverse momentum distribution of  $Z_1$  boson [i.e, with maximum  $P_T$ ] (left) and  $Z_3$  boson [i.e, with least  $P_T$ ] (middle) at the LHC for  $M_S = 3.5$  TeV and  $d = 3$ . Rapidity distribution of that  $Z_1$  boson (right) at the LHC for  $M_S = 3.5$  TeV and  $d = 3$  in the region where  $P_T^{Z_1} \in (900, 1400)$  GeV.

different we choose to use the invariant mass distribution of the identical di-bosons as it would be a better discriminator in the region of interest. We have also studied the dependency of the ADD model parameter  $M_S$  and the number of extra dimensions  $d$  keeping the UV scale  $\Lambda = M_S$ . In addition we have reported the sensitivity of the choice of  $\Lambda$  by varying it from  $\Lambda = 0.9M_S$  to  $0.95M_S$ . We have also studied the dependence of our LO predictions on the factorisation scale.

## Acknowledgments

The work of M.C.K. has been supported by Deutsche Forschungsgemeinschaft in Sonderforschungsbereich/Transregio 9 and by the European Commission through contract PITN-GA-2010-264564 (LHCPhenoNet). The work of V.R. has been partially supported by funds made available to the Regional Centre for Accelerator based Particle Physics (RECAPP) by the Department of Atomic Energy, Govt. of India. S.S. would like to thank UGC, New Delhi for financial support.

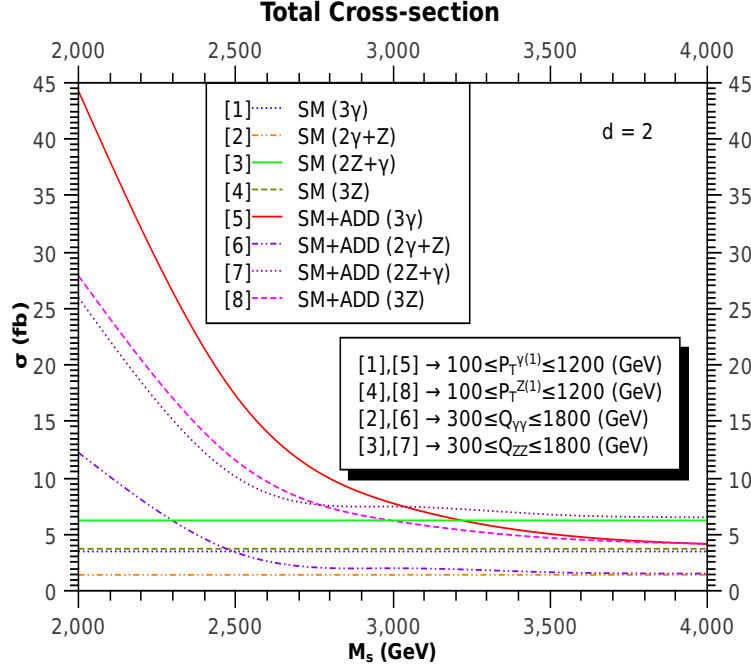


Figure 8: The total cross section for all the triple neutral gauge boson as a function of the extra dimension scale  $M_S$  for number of extra dimensions  $d = 2$ . The horizontal lines corresponds to the various SM contribution.

## References

- [1] N. Arkani-Hamed, S. Dimopoulos and G. Dvali, Phys. Lett. B 429 (1998) 263; I. Antoniadis, N. Arkani-Hamed, S. Dimopoulos and G. Dvali, Phys. Lett. B 436 (1998) 257; N. Arkani-Hamed, S. Dimopoulos and G. Dvali, Phys. Rev. D59 (1999) 086004.
- [2] G. F. Giudice, R. Rattazzi, and J. D. Wells, Nucl. Phys. B544 (1999) 3.
- [3] T. Han, J. D. Lykken and R. J. Zhang, Phys. Rev. D59 (1999) 105006
- [4] J. L. Hewett, Phys. Rev. Lett. 82 (1999) 4765; Prakash Mathews, V. Ravindran, K. Sridhar and W. L. van Neerven, Nucl. Phys. B713 (2005) 333; Prakash Mathews, V. Ravindran, Nucl. Phys. B753 (2006) 1; M.C. Kumar, Prakash Mathews, V. Ravindran, Eur. Phys. J. C49 (2007) 599.
- [5] O. J. P. Eboli, Tao Han, M. B. Magro, P. G. Mercadante, Phys. Rev. D61 (2000) 094007; K.m. Cheung and G. L. Landsberg, Phys. Rev. D 62 (2000) 076003.
- [6] M.C. Kumar, Prakash Mathews, V. Ravindran, Anurag Tripathi, Phys. Lett. B672 (2009) 45; Nucl. Phys. B818 (2009) 28.

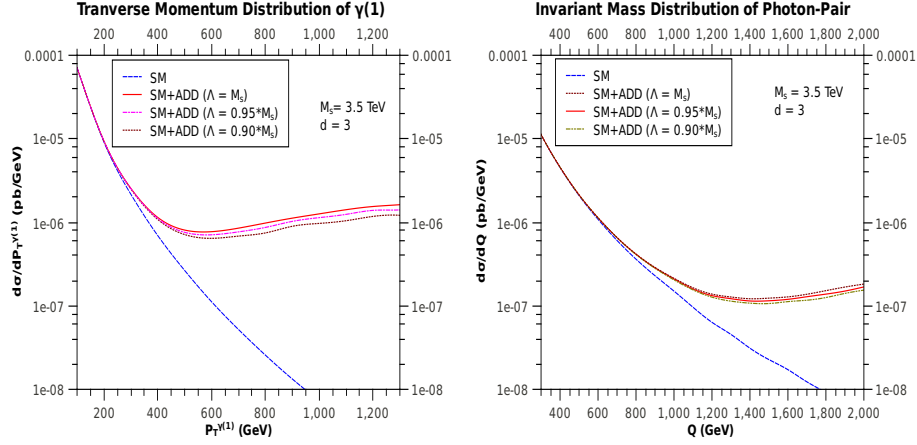


Figure 9:  $P_T^{\gamma(1)}$  distribution of the  $\gamma\gamma$  final state (left) and invariant mass distribution of the  $\gamma\gamma$  pair in the  $\gamma\gamma Z$  final state (right), for the cut off scale  $\Lambda = (0.9, 0.95, 1)M_S$ , where  $M_S = 3.5$  TeV and  $d = 3$ .

- [7] Neelima Agarwal, V. Ravindran, V. K. Tiwari, Anurag Tripathi, Nucl. Phys. B830 (2010) 248; Phys. Rev. D82 (2010) 036001.
- [8] Prakash Mathews, Sreerup Raychaudhuri, K. Sridhar, Phys. Lett. B450 (1999) 343; JHEP 0007 (2000) 008.
- [9] E. A. Mirabelli, M. Perelstein and M. E. Peskin, Phys. Rev. Lett. 82 (1999) 2236; S. Karg, M. Karämer, Q. Li, D. Zeppenfeld, Phys. Rev. D81 (2010) 094036; X. Gao, C. S. Li, J. Gao, J. Wang, Phys. Rev. D 81 (2010) 036008; M. C. Kumar, Prakash Mathews, V. Ravindran, Satyajit Seth, Nucl. Phys. B847 (2011) 54; J. Phys. G38 (2011) 055001.
- [10] J. M. Campbell, J. W. Huston, W. J. Stirling, Rep. Prog. Phys. 70 (2007) 89.
- [11] M. Golden, S. R. Sharpe, Nucl. Phys. B261 (1985) 217.
- [12] V. Barger, T. Han, Phys. Lett. B212 (1988) 117.
- [13] T. Binoth, G. Ossola, C. G. Papadopoulos, R. Pittau, JHEP 0806 (2008) 082.
- [14] A. Lazopoulos, K. Melnikov, F. Petriello, Phys. Rev. D 76 (2007) 014001.
- [15] G. Bozzi, F. Campanario, V. Hankele, D. Zeppenfeld, Phys. Rev. D 81 (2010) 094030.
- [16] G. Bozzi, F. Campanario, M. Rauch, D. Zeppenfeld, Phys. Rev. D 84 (2011) 074028.
- [17] CMS Collaboration, Report No. CMS-PAS-SUS-09-004, 2009.

- [18] A. Zerwekh, C. Dib, and R. Rosenfeld, Phys. Lett. B 549 (2002) 154.
- [19] M. C. Kumar, Prakash Mathews, V. Ravindran, Satyajit Seth in preparation.
- [20] J. A. M. Vermaseren, math-ph/0010025.
- [21] J. Pumplin et. al., JHEP 07 (2002) 012.
- [22] CMS Collaboration, arXiv: 1112.0688 [hep-ex]
- [23] ATLAS Collaboration, arXiv: 1112.2194 [hep-ex]
- [24] M. C. Kumar, Prakash Mathews, V. Ravindran, Satyajit Seth in preparation.